euronoise

Prediction of the Sound Transmission Loss of Multi-layered Small Sized Elements

Stefan Schoenwald[a], Eddy Gerretsen[b] and Heiko Martin[a]

[a]Eindhoven University of Technology, Den Dolech 2, BWK/BPS, 5600 MB Eindhoven, Netherlands
[b]TNO Science and Industry, Stieljesweg 1, 2628CK Delft, Netherlands
s.schoenwald@tue.nl

In this paper an improved method for the prediction of the sound transmission loss of multilayered finite structures, like glazing will be presented.
The sound transmission loss of an infinite structure is predicted with a common transfer matrix as a function of the angle of the incident sound wave. Then Villiot's spatial windowing method is applied to take into account the finiteness of the element. Usually an ideal diffuse distribution of the incident sound power is assumed and the prediction results are integrated over all angles of incidence. The obtained prediction results tend to underestimate sound transmission loss due to the dominance of the small values for gracing incidence. Often simple ad-hoc corrections are used for improvement, like Beranek's field incidence, that fail for multilayered structures. Kang suggests that the incident sound power on a surface of a room generally is Gaussian distributed on the angle of incidence and introduces a weighting function for the integration of the prediction results over the angles of incidence.
New in this paper is that spatial windowing as well as a Gaussian distributed sound power is considered for the prediction of the transmission loss. The results of the prediction are validated by experiment.

1 Introduction

Often an estimate of the sound reduction index of a double or multiple leaf flat partition is necessary and measurement data is not available.

Usually a simple transfer matrix approach for an infinite structure is applied for the prediction of the sound reduction index but the results often are not satisfactory and underestimate the performance of the partition in comparison to experiment. In reality the size of the considered elements is not infinite and the directional distribution of the energy in the incident sound field is not uniform. Further the mineral wool that is used as absorbent in the cavity is usually not isotropic and the flow resistivity is different in direction normal and perpendicular to the surface of the bats.

In this paper all these aspects are taken into account and an improvement of the prediction results is achieved when existing methods are combined.

2 Transfer matrix method

In this paper double leaf panels are considered as it is shown figure 1. Two flexible plates (plate 1 and plate 2) are separated by a cavity that can be either empty, partly filled or completely filled with an absorbent material and hence three fluid regions (region II to region IV) are defined in the cavity that can have different material properties. The leaves are only coupled fluid dynamically across the cavity and structural connections are neglected.

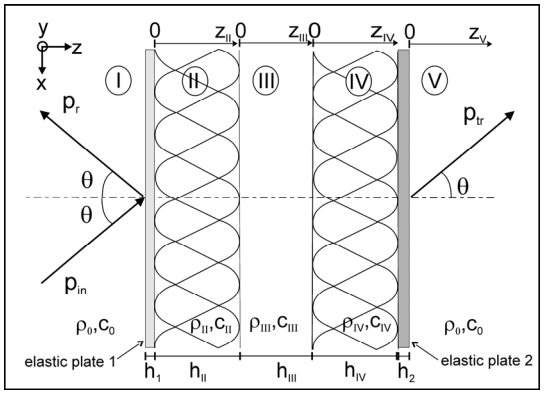

Fig.1 Double leaf panel in the transfer matrix approach

2.1 Fluid regions

The five fluid regions in the model are denoted with roman numbers and waves in the fluid have to fulfil the Helmholtz equation. In the following the two dimensional case is considered since all materials have the same properties in the x- and y- direction. The general solution for the sound pressure $p_r(x, z_r)$ in region r is given by equation 1.

$$p_r(x,z_r) = \left(a_{r+}e^{-ik_{zr}z_r} + a_{r-}e^{ik_{zr}z_r}\right)e^{-ik_x x} \quad (1)$$

Equation 1 is valid for all fluid regions - except of region V in the receiving room - since a propagating wave component in positive and negative z-direction is assumed to take into account the reflections at the interfaces of the regions. In fluid region V only the first term in the bracket is used since only an outgoing sound wave in positive z-direction is assumed. The time dependence $e^{i\omega t}$ is omitted for the matter of simplicity in all solutions. a_{r+} and a_{r-} are the unknown amplitudes of the two waves. k_{zr} and k_x are the wavenumber components in x- and z-direction. k_x is the so-called trace wavenumber of the sound wave that is incident in region I under the declination angle θ and depends on the natural wavenumber of the fluid in region I which is air in the considered case. k_x is equal for all fluid regions and all flexible plates.

$$k_x = k_0 \cdot \sin(\theta) \quad (2)$$

$$k_{zr} = \sqrt{k_r^2 - k_x^2} \quad (3)$$

The wavenumber component k_{zr} in z-direction depends on the trace wavenumber k_x and the natural fluid wavenumber k_r of region r.

2.2 Flexible plates

The leaves are considered as thin plates and the general solution of the bending wave has to fulfil the Kirchhoff equation and the normal plate displacement $w_p(x)$ of plate p is given by equation (4).

$$w_p(x) = a_p e^{-ik_x x} \quad (4)$$

In the plates of course wave propagation is only possible in x-direction and again the wavenumber k_x is equal to the trace wavenumber of the incident wave.

2.3 Modelling of the absorbent

In the cavity of building element usually mineral wool bats are used as absorbent that are not bounded to the surfaces of the leaves nor exhibit strong flexural properties. Hence only wave propagation in the fluid phase is taken into account and structural wave propagation in the solid frame is neglected. Thus it is not necessary to apply Biot's theory for the modelling of the absorbent and it can be considered as dissipative fluid with a complex wave speed $\underline{c}_r$ and effective complex fluid density $\underline{\rho}_r$ that are given as function of the flow resistivity Ξ by e.g. Delany and Bazley [1].

Unfortunately often only the minimal requirement is given as nominal value for the flow resistivity that are measured with a steady airflow in direction normal to the surface of the bats. In this thesis the absorption coefficient for normal sound incidence is measured at small sized samples that have been cut out of the used bats in direction normal and parallel to the surface.

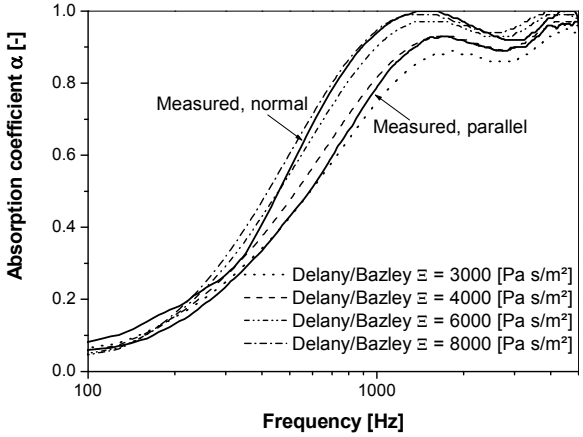

Fig.2 Absorption coefficient α of mineral wool samples (h = 60 mm) measured in an impedance tube and predicted by Delany and Bazley (samples cut normal and parallel to the surface out of the bat)

The measured absorption coefficient is shown in figure 2 and obviously is different in both orthogonal directions due to the layered consistency of the material. The absorption coefficient further depends on the flow resistivity that has to be different in both orthogonal directions respectively. Absorption coefficients that are predicted according to [1] agree well if a flow resistivity between 6 kPa s/m^2 and 8 kPa s/m^2 is assumed in normal direction and between 3 kPa s/m^2 and 4 kPa s/m^2 in parallel direction to the surface of the bats. Thus in the transfer approach the flow resistivity and the complex group velocity $\underline{c}_r(\theta_r)$ is assumed to be a continuous function of the propagation direction θ_r of the sound wave in region r.

$$\underline{c}_r(\theta_r) = \underline{c}_{r,x} \cdot \sin(\theta_r) + \underline{c}_{r,z} \cdot \cos(\theta_r) \quad (5)$$

$\underline{c}_{r,x}(\theta_r)$ and $\underline{c}_{r,z}(\theta_r)$ is the complex wave speed in the two orthogonal directions that are given by Delany and Bazley as function of the flow resistivity in the two directions. Wavenumber component k_x in the absorbent is also equal to the trace wavenumber of the incident wave. Thus the direction of wave propagation in the absorbent is given by equation 6 and the wavenumber component $k_{r,z}$ in z-direction by equation 7.

$$\tan(\theta_r) = \frac{\underline{c}_{r,z}}{\frac{\omega}{k_x} - \underline{c}_{r,x}} \quad (6)$$

$$k_{r,z} = \frac{\omega}{\underline{c}_r(\theta_r)} \cdot \cos(\theta_r) \quad (7)$$

2.4 Boundary conditions and transfer matrix

The unknown wave amplitudes and the particular solutions of the wave equations are determined by the boundary conditions at the interfaces of the fluid regions and at the plate surfaces. At the plate surfaces the inhomogeneous Kirchhoff equation 8 has to be fulfilled and the normal plate displacement p has to be equal to the particle displacement in z-direction in the fluid regions on both sides.

$$\left[\underline{B'}_p \nabla^2 - m''_p \omega^2\right] w_p(x) = p_r(x, z_r = h_r) - p_{r+I}(x, z_{r+I} = 0) \quad (8)$$

$$w_p(x) = w_r(x, z_r = h_r) \quad (9)$$

$$w_p(x) = w_{r+I}(x, z_{r+I} = 0) \quad (10)$$

∇^2 is the two dimensional Laplace operator, $\underline{B'}_p$ is the complex bending stiffness of the plate p and m''_p is its mass per unit area. The particle displacement is proportional to the derivative of the sound pressure and is given by the Euler equation 11. $\rho_{z,r}$ is the effective fluid density for wave propagation in z-direction.

$$w_{z,r} = \frac{1}{\omega^2 \rho_{z,r}} \frac{\partial p_r}{\partial z_r} \quad (11)$$

At the interface of two fluid regions the continuity condition for the particle displacement in z-direction and the equilibrium condition for the sound pressure has to be fulfilled.

$$w_{z,r}(x, z_r = h_r) = w_{z,r+I}(x, z_{r+I} = 0) \quad (12)$$

$$p_r(x, z_r = h_r) = p_{r+I}(x, z_{r+I} = 0) \quad (13)$$

The boundary conditions determine a set of linear equations that define the transfer matrix. Further the wave amplitude a_{I+} of the incident wave in the source region I is set to unity for the matter of simplicity. The system is well defined since the number of equations is equal to the number of unknown wave amplitudes. The complete transfer matrix for the considered model is presented in [2].

If the fluids in region I and in region V on both sides of the partition are equal than the sound transmission coefficient $\tau_{inf,\theta}(\theta)$ of the infinite plate for an oblique angle of incidence θ is simply given as the ratio of transmitted to incident sound intensity I or by the magnitude of the wave amplitudes of the corresponding sound waves respectively.

$$\tau_{\inf,\theta} = \frac{I_{tr}}{I_{in}} = \frac{|a_{V+}|^2}{|a_{I+}|^2} = \quad (14)$$

3 Spatial windowing

So far the sound transmission coefficient $\tau_{inf,\theta}(\theta)$ for an infinite partition and for an oblique angle of incidence is predicted. With Villot's spatial windowing method it is possible to determine the sound transmission coefficient $\tau_{fin,\theta}(\theta)$ of a finite panel with dimensions l_x by l_y from the results of the transfer matrix method [3]. An infinite structure is assumed that is on one side partially excited by airborne sound over a finite area of size S and also only radiates sound by this area on the other side of the structure as it is shown in figure 3.

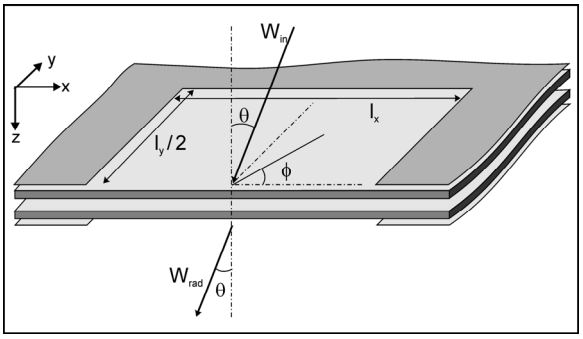

Fig.3 Spatial windowing – sound transmission and radiation from partially excited partitions

$$\tau_{fin,\theta} = \tau_{\inf,\theta} \cdot \left[\sigma(k_0,\theta)\cdot\cos(\theta)\right]^2 \qquad (15)$$

The transmission coefficient $\tau_{fin,\theta}(\theta)$ of the finite plate is given by equation 15. The first factor on the right hand side is the transmission coefficient for an infinite structure and depends only on the properties of the panel. The second factor is the ratio of the non-resonant radiation efficiency $\sigma(k_0,\theta)$ of a finite plate and of an infinite plate. It is a function of the plate geometry and the angle of incidence only. Novak [4] gives $\sigma(k_0,\theta)$ for this situation in terms of a triple integral over the Fourier components α and β and the azimuth angle ϕ.

$$\sigma(k_0,\theta) = \frac{2k_0}{\pi^3 S}\int_0^{2\pi}\iint_{\alpha\beta}\frac{1}{\sqrt{k_0^2-\alpha^2-\beta^2}} \left(\frac{\sin\left((\alpha-k_x)\cdot 0{,}5l_x\right)}{(\alpha-k_x)}\frac{\sin\left((\beta-k_y)\cdot 0{,}5l_y\right)}{(\beta-k_y)}\right)^2 d\alpha\, d\beta\, d\phi \qquad (16)$$

with:

$$\alpha^2+\beta^2 < k_0^2$$

$$k_x = k_0\sin\theta\cos\phi$$

$$k_y = k_0\sin\theta\sin\phi$$

The integration is performed over all possible azimuth angles ϕ since the plate dimensions are different in x- and y-direction. The sound transmission coefficient of the transfer matrix approach on the other hand is independent from this angle since a two-dimensional case is considered. The remaining double integral has to be evaluated over all combinations of Fourier components that lay inside a circle with the radius k_0. In this paper integration is performed numerically over all integrals with a commercial software package and the non-resonant radiation efficiency is determined independently from the considered panel for the same set of discrete frequencies and declination angles θ like the sound transmission coefficient $\tau_{inf,\theta}(\theta)$.

4 Averaging over declination angle θ

The transmission coefficient $\tau_{fin,\theta}(\theta)$ has to be averaged further over the declination angles θ since in reality usually a diffuse sound field exists on the source side. Waves are incident on the partition under all possible angles and the statistical transmission coefficient τ_{fin} for a diffuse sound field is given by the so-called Paris' formula.

$$\tau_{fin} = \frac{\int_0^{\pi/2}\tau_{fin,\theta}(\theta)\sin(\theta)\cos(\theta)\,G(\theta)\,d\theta}{\int_0^{\pi/2}\sin(\theta)\cos(\theta)\,G(\theta)\,d\theta} \qquad (17)$$

$G(\theta)$ is a weighting function to take into account the directional distribution of sound power in the incident sound field. In case of an ideal diffuse field with an equal probability of incident sound waves from all directions it is set to unity for all angles of incidence. Since for this distribution the predicted sound transmission coefficient is usually overestimated in comparison to measurement results, Beranek suggested an ad-hoc correction that is called field incidence case. A good agreement between predicted and measured single number quantities is found if $G(\theta)$ is assumed to be unity below a cut-off angle $\theta_{cut\text{-}off}$ of about 78° and for bigger values it is set to zero. Kang [5] investigated the directional distribution of incident power on surfaces of rooms of different shape with ray-tracing models. He found that for reverberant chambers the Gaussian distribution of equation 18 approximates the directional distribution of the incident power best if β is in the range between 1 and 2.

$$G(\theta) = e^{-\beta\theta^2} \qquad (18)$$

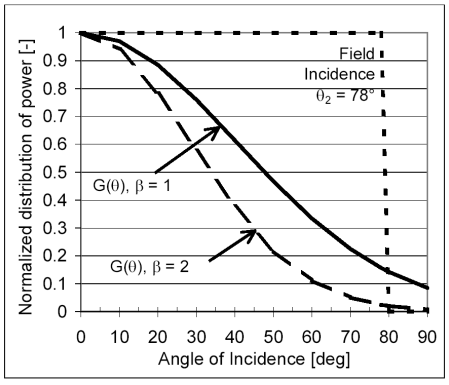

Fig.4 Weighting function $G(\theta)$ for the directional distribution of the sound power in the incident sound field

The different weighting functions for the sound power are presented in figure 4. Kang's Gaussian distribution assumes that the probability of sound waves close to grazing incidence is less than of sound waves close to normal incidence. In this paper the transmission coefficients are calculated for a discrete set of angles of incidence and the integral in equation 17 is replaced by a summation.

5 Measurement set-up

Measurements are carried out in the transmission test facility of the Acoustics Laboratory of Eindhoven University of Technology. Originally the facility is designed for testing of wall structures and fulfils the requirements of ISO 140-1. A double leaf filler wall of heavy calcium silicate blocks (2x 0,20 m) is placed in the big test opening (10 m²) separating the two chambers to form a small test opening (1,25 m x 1,50 m) for glazing according ISO 140-1, Annex C.

5.1 Measurement methods

The sound reduction index R – which is the logarithmic inverse of the transmission coefficient - is measured according ISO 140-3. Two fixed loudspeakers driven uncorrelated with white noise are used for excitation of the sound field in the source room and the sound pressure is measured in both chambers simultaneously with two rotating microphone booms. The reverberation time in the receiving room is determined from three measured sound pressure level decays at three fixed microphone positions.

5.2 Test specimens

Two test specimens are considered in this paper. The first specimen "LvA1" is a simple double glazing consisting of two leaves of 6 mm float glass that are separated by a 16 mm deep cavity that is filled with air. The glazing is mounted in one leaf of the filler wall using wooden battens according to ISO 140-3.

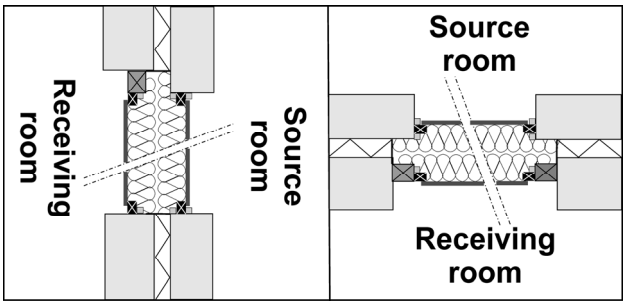

Fig.5 Test specimen "LvA2" – double leaf gypsum board on two wooden frames with no structural connections between the leaves (left: vertical cut; right: horizontal cut)

The second test specimen "LvA2" consists of two equal sized gypsum boards (thickness 12 mm, Type GKB, m''=8,64 kg/m², B'=380 Nm) that are screwed at their edges to wooden frames. One frame is mounted like the glazing in the leaf of the filler wall that is exposed to the source room and the second frame is mounted in the second leaf of the filler wall. Since the test opening in the second leaf is bigger, rigid wooden beams are bolted to the reveal of the opening to adjust its size. Between the two panels and also between the leaves of the filler wall no structural connections exist and sound transmission occurs through the panel only by coupling across the cavity. The cavity (depth 0,18 m) is filled with two layers of 60 mm mineral wool as it is shown in figure 5. All joints between the two specimens and the filler wall are sealed or taped to suppress sound leaks.

6 Comparison of prediction and measurement

The measurement results of the two specimens are used to validate the prediction methods. Specimen "LvA1", namely the glazing, is used to show the effect of spatial windowing and the different weighting functions for the directional distribution on the predicted sound reduction index. For specimen "LvA2" the improvement of the prediction results relative to measurement result is shown when flow resistivity of the absorbent is assumed to be angle dependent. The predictions are carried out for a set of discrete frequencies with a spacing of 1 Hz and declination angles with a spacing of 0,25°. The results are band filtered at the end to obtain third octave band values.
Below coincidence frequency the applied prediction method – namely the transfer matrix approach in combination with the spatial windowing - takes into account only non-resonant sound transmission and at and above coincidence frequency the resonant component. Hence the two test specimens are chosen for validation of the method because the non-resonant transmission component dominates below coincidence frequency.

6.1 Distribution of energy

Five prediction results of the sound reduction index R of specimen "LvA1" are presented in figure 6. The first is referred to "Diffuse – infinite" and the sound reduction index of an infinite panel obtained with the transfer matrix method is averaged over all angles of incidence with the weighting function set to unity like for an ideal diffuse sound field. It underestimates the sound reduction index by more than 10 dB in comparison to measurement in most of the frequency range. Only in the range above coincidence frequency it approaches the measurement results and overestimates the sound reduction index slightly like the remaining prediction results.

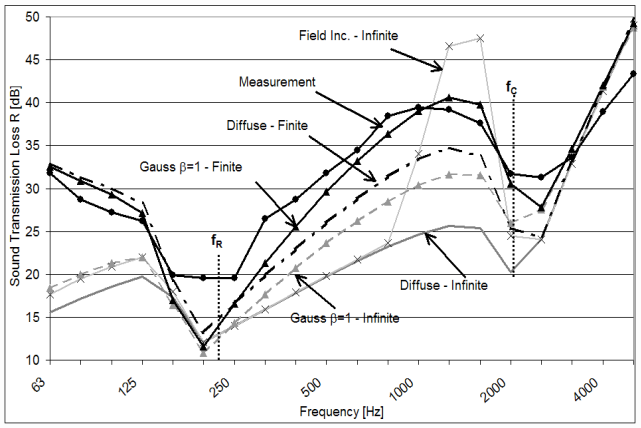

Fig.6 Sound reduction index R of a double glazing (float glass: 6 mm; air: 16 mm; float glass: 6 mm)

In the second prediction also an infinite plate is considered but direction averaging is done according to according Beranek's field incidence case. In the low and high frequency

range it approaches the result of the diffuse field case but in the middle frequency range the prediction results increase and overestimate the measured sound reduction index R grossly. Above 1000 Hz the mass-spring-mass resonance is caused by sound waves that are incident with angles bigger than the cut-off angle for averaging. Hence the small sound reduction index around this resonance is not taken into account for direction averaging above 1000 Hz and the sound reduction index increases strongly. The spectrum does not match the spectrum of the measurement results but the agreement of the single number value that is not shown in this paper is certainly sufficient due to the under- and overestimation in part of the frequency range. If Kang's Gaussian weighting function is taken into account with parameter β set to unity then the prediction result for an infinite plate is bigger in the middle frequency range than for ideal diffuse field but the difference to the measurement result is still about 10 dB. In the low and high frequency range this prediction also approaches the result of the diffuse field.

If spatial windowing is applied - the results are referred to "finite" - then the sound reduction index is bigger below coincidence frequency f_c. in comparison to the infinite panel. Below the fundamental mass-spring-mass resonance frequency f_R the difference to measurement result is even less than 3 dB but in the middle frequency range it still exceeds 5 dB for an ideal diffuse sound field. If further the Gaussian distribution of incident sound power is considered then in the range below the fundamental resonance frequency the result does not change in comparison to a diffuse field. However, in the middle frequency range it increases further and the agreement to measurement is good. The difference is less than 3 dB except at and close to the fundamental resonance frequency f_R. This difference is caused by the damping of the resonance due to the connections of the glass plates at their edges that is not taken into account in the prediction model.

6.2 Flow resistivity of absorbent

The sound reduction index R of the specimen "LvA2" is predicted with the transfer matrix approach, spatial windowing as well as the Gaussian distribution (β=1) of incident sound power is taken into account and the influence of the modelling of the absorbent in the cavity on the prediction results is further investigated.

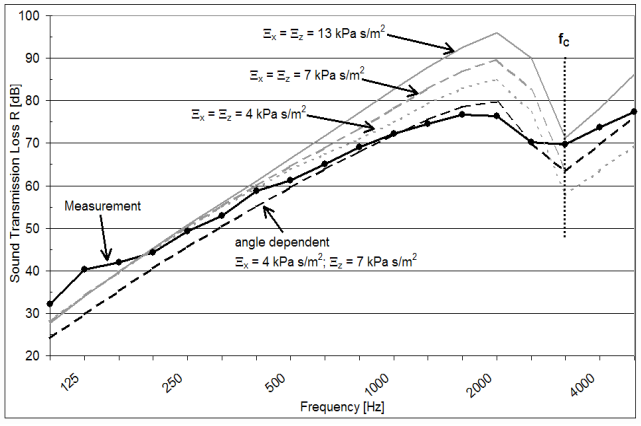

Fig.7 Sound reduction index R of the double leaf gypsum panel "LvA2" (prediction with different modelling of the absorbent in the cavity)

Four prediction results are presented, three with an absorbent with isotropic material properties and one with an angle dependent flow resistivity of the absorbent. For the isotropic cases the flow resistivity is assumed to be equal in all directions and to be 13 kPa s/m² (according manufacturer), 7 kPa s/m² (measured normal to surface) and 4 kPa s/m² (measured parallel to surface). All prediction results for the isotropic case overestimate the sound reduction index just below coincidence frequency f_c and either over- or underestimate it above this frequency. Further if an angle dependent flow resistivity is assumed that is 7 kPa s/m² normal and 4 kPa s/m² parallel to the surface of the bats then the agreement of prediction and measurement results is good in most of the frequency range. The difference is less than 3 dB and only in the low frequency range above the mass-spring-mass resonance it increases slightly like at the glazing due to neglecting the damping of the resonance in the prediction model.

7 Conclusion

In this paper it has been shown that it is possible to get a good estimate of the sound reduction index R of small sized double leaf panels with a common transfer matrix approach. The finite size of the considered structure has to be taken into account by applying the spatial windowing method and further the directional distribution of incident sound has to be assumed to be Gaussian. In this case the difference between prediction and measurement results has been less than 3 dB in most of the frequency range except around the mass-spring-mass frequency due to neglecting the damping at the supports at the plate edges. Fibrous absorbent in the cavity, like e.g. mineral wool, can be incorporated in the transfer matrix approach simply by considering only wave propagation in the fluid phase and assuming a complex wave speed and a complex effective fluid density. However, usually the flow resistivity of mineral wool is different in normal and parallel direction to the surface of the bats and has to be assumed in the transfer matrix as a function of the propagation direction of the sound wave in the absorbent.

References

[1] Delany, M.E., Bazley, E.N.: Acoustical properties of fibrous absorbent materials. Applied Acoustics, 3(2) (1970), 105-116

[2] Schoenwald, S.: Doctoral Thesis, Eindhoven University of Technology, exp. august 2008

[3] Villot, M. et al.: Predicting the acoustical radiation of finite size multi-layered structures by applying spatial windowing on infinite structures. Journal of Sound and Vibration 245(3) (2001), 433-455

[4] Novak, R.A.: Radiation of partially excited plates. Acta Acustica 3 (1995), 561-567

[5] Kang, H.-J.: Prediction of sound transmission loss through multilayered panels by using Gaussian distribution of directional incident energy. Journal of the Acoustical Society of America 107(3) (2000), 1413-1420